A Novel Cooling System to Reduce Thermally-Induced Errors of Machine Tools

M.A. Donmez, M.H. Hahn, J.A. Soons
Manufacturing Engineering Laboratory
National Institute of Standards and Technology, Gaithersburg, USA
Submitted by J. Bryan (1), Pleasanton, USA

Abstract
This study explores a method to reduce thermally-induced errors of machine tools through temperature stabilization with compressed air. The method uses inexpensive, specially-shaped, silicon tubing with small slits. Compressed air forced through such tubing increases heat dissipation from the surface through Coanda-effect cooling. This paper describes experiments performed on a simulated heat source as well as a turning center to evaluate and improve the effectiveness of the method. The results show that this system, which can easily be applied to existing machines, can significantly reduce thermal drift and may be a viable alternative to other methods to reduce thermally-induced errors.

Keywords:
Machine, Thermal, Error

1 INTRODUCTION

Temperature gradients in machine tool structures due to various different heat sources are known to result in expanded and warped machine elements, which in turn affect positioning, straightness, angular, and alignment errors. In fact, studies carried out over the last four decades indicated that about 40% to 70% of the errors degrading the accuracy of machine tools are thermally induced [1,2,3]. Methods to reduce thermally-induced errors that have been reported in the literature can be classified into three categories [1-12]:

- Decreasing temperature variations, for example, through cooling, improved environmental temperature control, or good operating practices such as spindle warm up.

- Decreasing the sensitivity of the machine tool structural loop to temperature variations, for example, through the use of symmetry in machine design, use of materials with a low thermal expansion, and isolation of heat sources.

- Compensating the errors, for example, by additional hardware or software, through a model that predicts errors in the relative position of the tool and work piece as a function of temperature changes during machine operation.

This study focuses on decreasing temperature variations by removing the heat at a location close to its source. Heat removal from major heat sources such as drive motors and spindles is usually obtained by convection. A more effective way to remove the heat is by forcing a large flow of temperature-controlled liquid around the heat sources [6, 7]. However, applying a liquid shower or cooling coil to an existing machine may be both difficult and costly. An alternative approach of an air shower system often suffers from poor heat transfer between air and machine components and poor accessibility through various structural elements.

This paper summarizes an investigation of the effectiveness of Coanda-effect cooling devices to remove heat from machine tool heat sources and to reduce thermally-induced errors.

2 COANDA-EFFECT COOLING DEVICES

The Coanda effect is the tendency of a fluid to cling to the surface that is near the orifice or nozzle from which the fluid emerges, creating a primary stream. In Coanda-effect cooling devices the primary stream acts as a fluid-powered fan and drags along a secondary stream of fluid that can be much (up to 20 times) larger than the primary stream, increasing the cooling effect [13].

In this study, we used commercially available soft silicon extrusion tubing with small, perforated slits as shown in Figure 1. This is also known as Personal Air Conditioning (PAC) tubing. When compressed air is applied to this tubing, the air escapes through the slits and, clinging to the surface of the lips, creating a primary stream.
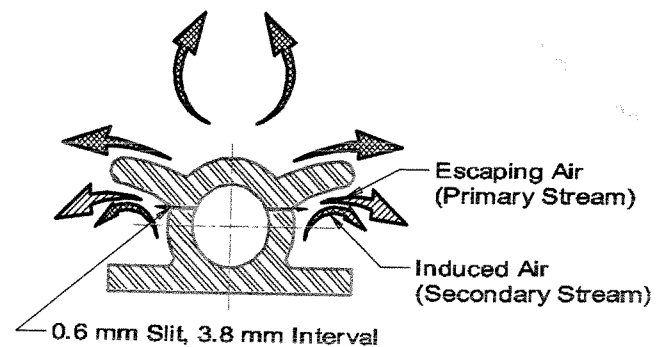

Escaping Air (Primary Stream)

Induced Air (Secondary Stream)

0.6 mm Slit, 3.8 mm Interval

Figure 1: Cross section of the Coanda-effect tubing used in this study.

2.1 Simulated cooling experiments

In order to characterize the cooling performance of the PAC tubing, we conducted experiments with a simulated drive motor consisting of a 140 mm diameter hollow aluminium cylinder with a foil heater attached to the inside surface of the cylinder. The cylinder was filled with foam insulation to ensure unidirectional heat flow. The tubing was spirally wrapped around the outer surface of the cylinder. Compressed air (about 600 kPa pressure) was circulated through the tubing to generate a Coanda effect. The surface temperature rise as a function of heat input via electrical power was measured using twelve thermocouples at 5 min intervals until it reached a steady

state. Steady-state temperatures were used to determine the effective heat transfer.

The total heat loss from the cylinder consisting of both convective and radiative heat transfer can be expressed as [14]:

$$P = P_c + P_r \approx (h_c + h_r)A\Delta T \qquad (1)$$

Where P is the electrical power input (W)

  P_c is heat loss by convection (W)

  P_r is heat loss by radiation (W)

  h_c is the convection coefficient (Wm^{-2}K^{-1})

  h_r is the radiation coefficient (Wm^{-2}K^{-1})

  A is surface area of cylinder (m^2)

  $\Delta T = T_s - T_a$

  T_s is the average surface temperature (K)

  T_a is the ambient temperature (K)

The radiative heat transfer is given by:

$$P_r = \varepsilon\sigma A(T_s^4 - T_a^4) \approx 4\varepsilon\sigma T_m^3 A\Delta T = h_r A\Delta T \qquad (2)$$

Where ε is the total emissivity of radiating surface

  σ is the Stefan-Boltzmann constant

  $T_m = (T_s + T_a)/2$

We measured the emissivity using a radiometer and calculated the radiative heat transfer. The convective heat loss was then calculated using equation (1).

We carried out experiments with four types of tubing: 5 mm diameter standard flow (SF) and 8 mm diameter high flow (HF), which had slits close to the upper lips, as well as ones with slits close to lower flanges designated as the new design (NSF and NHF). We also investigated the effect of the air temperature on the convection performance by attaching a vortex device to reduce the temperature of the inlet air to about 15 °C. Finally, in order to investigate the effects of the spacing between the tubing, we used four pitch spacings (40 mm, 50 mm, 75 mm, and 100 mm).

A typical result of the measurements is shown in Figure 2, where the temperature rise is plotted against the convective heat loss calculated using equations (1) and (2). In such a plot, the slope of the curve is the indication of the effective convection coefficient (1/h). A lower slope indicates a more effective cooling. The non-zero intercepts observed in the plot are due to the effects of mixing the air temperature coming out of the tubing with the actual ambient temperature. Figure 2 indicates no significant effect of pitch spacing in the cooling behavior.
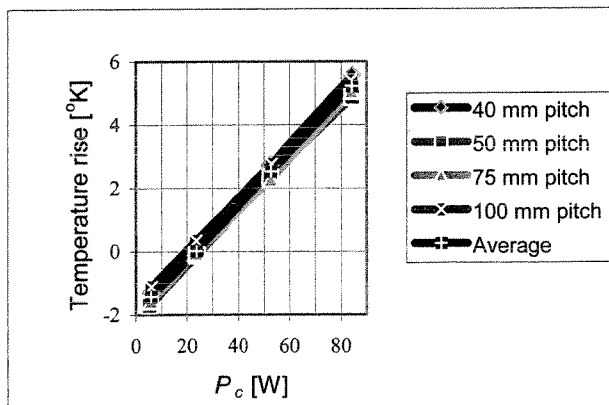

Figure 2: Test results using NSF tubing with vortex device for four different pitch spacing.

We also compared the effectiveness of PAC tubing against traditional forced convection and natural convection. For the case of forced convection, we used a blower placed in front of the cylinder blowing air at three different air speeds (1.7 m/s, 2.6 m/s, and 3.4 m/s). The summary of results, shown in Figure 3, indicates that PAC tubing improves the average convection coefficient by more than fifteen times compared to natural convection (indicated by 'NC' in Figure 3) and more than three times compared to forced convection by blower (indicated by 'FC' in Figure 3, averaged over three air speeds). Note that 'AVE' in Figure 3 indicates the average of the four tubing types.
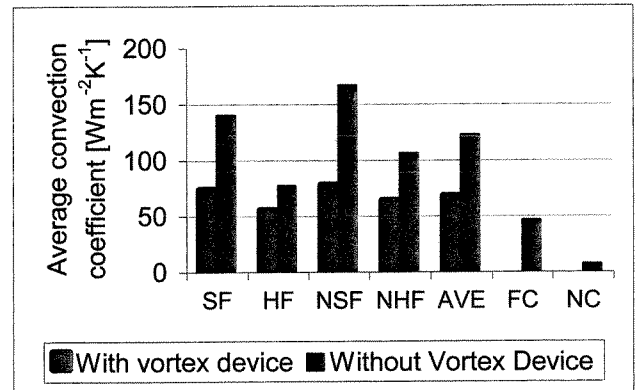

Figure 3: Summary of experiments with simulated heat source comparing cooling performance of Coanda-effect tubing against natural convection and forced convection.

2.2 Application to machine tools

In order to verify the effectiveness of Coanda-effect devices on reducing machine tool thermal deformations, we investigated a simple case of axial drift of a turning center spindle (rolling element bearing) with and without the PAC tubing. We wrapped the tubing around the headstock, from the spindle nose close to the front bearings to the spindle housing near the rear spindle bearing, with a total tubing length of 1660 mm (shown in blue in Figure 4). An additional 1430 mm long piece of tubing was wrapped around the hydraulic actuator of the collet closer, which is a significant heat source attached to the headstock, and then inserted into the spindle bore (shown in red in Figure 4). The test setup indicating the tubing arrangement is shown in Figure 4.
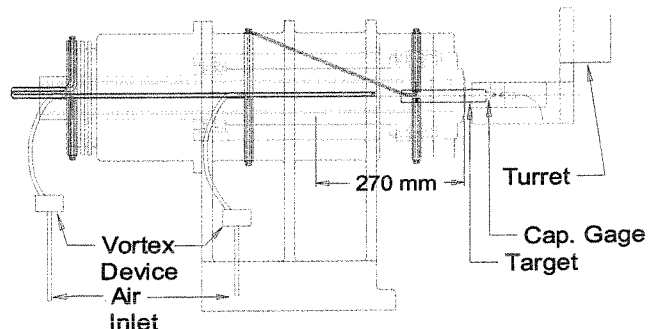

Figure 4: Experimental setup to measure axial spindle drift of turning center spindle.

For the axial spindle drift measurements, we used a capacitance gage, mounted on a fixture attached to the tool turret, located against a target artifact mounted on the spindle. We followed the procedures outlined in ISO 230-3 to determine axial spindle drift [15]. During the tests, in addition to supplied air pressure and the flow rate, we monitored temperatures at six locations: spindle nose, spindle housing close to front bearings, spindle housing close to rear bearing, hydraulic actuator housing

of the collet closer, ambient air, and the inlet air of the tubing. The estimated standard uncertainties for the measurements were: 0.2 °C for temperature, 20 kPa for air pressure, 6 L/min for air flow rate, and 0.02 μm for displacement (spindle drift). We ran the spindle at a constant speed of 210 rad/s (50% of maximum speed).

3 EXPERIMENTAL DESIGN

In order to examine the effects of various settings of PAC tubing on spindle axial drift, we designed statistical factorial experiments [16]. The settings (factors) considered were: tubing type with four levels (SF, HF, NSF, NHF), inlet air temperature with two levels (indicated by existence of vortex device), and air pressure with two nominal levels (high and low pressure). A full factorial design requires a minimum of 16 experiments (4x2x2) with additional baseline runs without using any tubing. However, during the preliminary experiments outlined above, the effect of the vortex device at low pressure showed no beneficial effect on cooling performance. So, to simplify the experimental design, we eliminated the case of low air pressure with a vortex device. Two runs (replications) for each remaining setting were conducted in this reduced factorial design, totalling 18 runs. Following the fundamental design of experiments principles of blocking and randomizing as well as some practical constraints, we organized the runs into a sequence as shown in Table 1. It should be noted that the vortex device not only reduces the temperature of the inlet air, but also the effective air flow rate (see for example test numbers 16 and 17).

Test No	Test condition			
	Tubing type	Vortex device	Pressure [kPa]	Measured flow rate [L/min]
1	No tubing	no	0	0
2	SF	no	700	175
3	SF	yes	550	175
4	NHF	No	350	220
5	NHF	Yes	700	200
6	HF	No	350	240
7	HF	Yes	700	135
8	NSF	No	700	350
9	NSF	Yes	700	160
10	NSF	No	350	190
11	NSF	No	620	330
12	HF	Yes	700	130
13	HF	No	700	370
14	NHF	yes	700	130
15	NHF	No	600	330
16	SF	Yes	700	175
17	SF	No	350	200
18	No tubing	No	0	0

Table 1: Run sequence for the experiments

4 EXPERIMENTAL RESULTS

Typical results of measured temperatures and spindle axial drift corresponding to each experimental run are shown in Figures 5 and 6 respectively.

Spindle Nose ——— Front Housing ——— Rear Housing
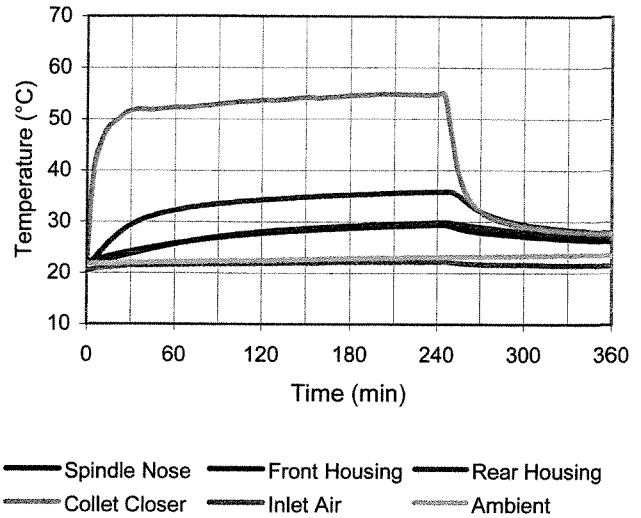——— Collet Closer ——— Inlet Air ——— Ambient

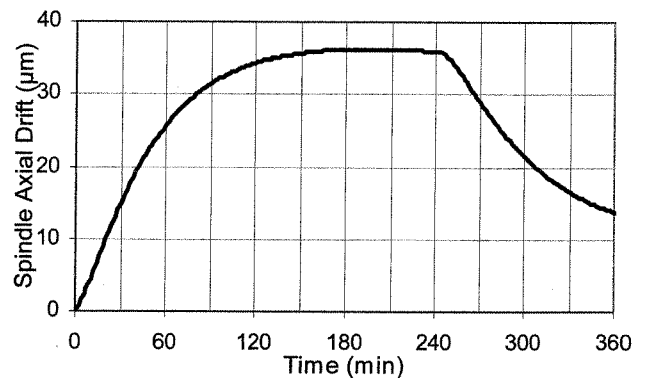Figure 5: Measured temperatures for Run # 17.

Figure 6: Measured axial spindle drift for Run # 17.

The results of the statistical analysis, which are shown in Figure 7, indicate that PAC tubing significantly decreases the amount of spindle axial drift. In this figure each data point corresponds to a test condition described in Table 1. Air pressure and air temperature do not indicate a statistically significant difference in the spindle axial drift. The best conditions resulting in the smallest spindle drift, which are marked with a red circle in the same figure, correspond to SF type tubing.
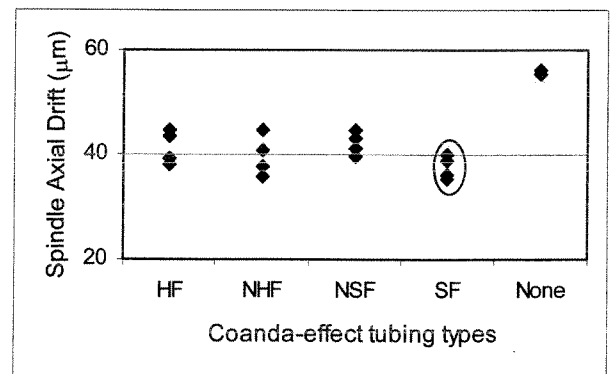

Figure 7: Graphical representation of axial spindle drift for various settings of tubing type.

Table 2 summarizes the test results averaged over the types of tubing used: SF, NSF, HF, and NHF. The averaged results show that in addition to a reduction in axial spindle drift, the time to reach the maximum drift is also reduced when PAC tubing is used.

Cases	vortex dev.	air pressure [kPa]	air flow rate [L/min]	axial drift [µm]	time to reach max drift [min]
No tubing				55.8	273
With tubing	yes	700	160	41.5	188
With tubing	no	350	210	40.2	180
With tubing	no	650	310	38.4	168

Table 2: Averaged test results for the various types of tubing.

5 SUMMARY

We evaluated the efficiency of a novel cooling system, Coanda-effect tubing, to reduce the thermal drift of a spindle. An average of 30% improvement in spindle drift was observed. The best case was observed (see Test No 16 in Table 1) with SF type tubing (175 L/min flow rate) at 700 kPa air pressure without any vortex device, reducing the axial drift by 20 µm (36%) and the time to reach the maximum drift by approximately 100 minutes (37%), compared to the case of no tubing. The power requirement for this application corresponding to the pressure and flow rate is 0.6 kW as calculated by [17]. Considering the pump efficiency and the need to keep the system on overnight to minimize thermal transients, the total operating cost of such cooling is about $ 2 per day (at a rate of $ 0.10/kWH).

Air-cooling normally is not as effective as liquid cooling to remove heat due to lower heat capacity of the medium. However, utilizing the Coanda effect improves the cooling performance of air and makes it a viable alternative to cool machine tool components for new and existing machines.

6 ACKNOWLEDGMENTS

7 DISCLAIMER

Certain trade names and company products are mentioned in the text or identified in an illustration in order to adequately specify the experimental procedure and equipment used. In no case does such an identification imply recommendation or endorsement by the National Institute of Standards and Technology, nor does it imply that the products are necessarily the best available for the purpose.

8 REFERENCES

[1] Bryan, J.B., 1968, International Status of Thermal Error Research, Annals of the CIRP, 16/2:203-215.

[2] Bryan, J.B., 1990, International Status of Thermal Error Research, Annals of the CIRP, 39/2: 645-656.

[3] Weck, M., McKeown, P.A., Bonse, R., Herbst, U., 1995, Reduction and Compensation of Thermal Errors in Machine Tools, Annals of the CIRP, 42/2: 589-598.

[4] Sugishita, H., Nishiyama, H., Nagayasu, O., Shin-Nou, T., Sato, H., Hori, O., 1988, Development of Concrete Machining Center and Identification of the Dynamic and the Thermal Structural Behaviour, Annals of the CIRP, 37/1: 377-380.

[5] Bryan, J.B., Donaldson, R.R., Clouser, R.W., McClure, R., 1972, A Practical Solution to the Thermal Stability Problem in Machine Tools, Society of Manufacturing Engineers MR-72-138, (also UCRL 73577).

[6] Bryan, J.B., Donaldson, R.R., Clouser, R.W., Blewett, W.H., 1973, Reduction of Machine Tool Spindle Growth, Proceedings of the 1st NAMRC Conference, Hamilton, Canada, May 14-15, 1973, (also UCRL 74672).

[7] Bryan, J., Carter, D., Clouser, W., Hamilton, J., 1982, Order of Magnitude Improvement in Thermal Stability using a Liquid Shower on a Measuring Machine, Precision Engineering Workshop, SME, St Paul, (also UCRL 87591).

[8] Donaldson, R., Patterson, S., 1983, Design and Construction of a Large Vertical Axis Diamond Turning Machine, SPIE 27th Annual Technical Symposium.

[9] Moriwaki, T., 1988, Thermal Deformation and its On-Line Compensation of Hydrostatically Supported Precision Spindle, Annals of the CIRP, 37/1:393-396.

[10] Moriwaki, T., Shamoto, E., 1998, Analysis of Thermal Deformation of an Ultraprecision Air Spindle System, Annals of the CIRP, 47/1: 315-319

[11] Donmez, M.A., Blomquist, D.S., Hocken, R.J., Liu, C.R., Barash, M.M., 1986, A General Methodology for Machine Tool Accuracy Enhancement by Error Compensation, Precision Engineering, Vol. 8, No. 4: 187-196.

[12] Hatamura, Y., Nagao, T., Mitsuishi, M., Kato, K., Taguchi, S., Okumura, T., Nakagawa, G., Sugishita, H., 1993, Annals of the CIRP, 42/1:549-552.

[13] Reba, I., 1966, Applications of Coanda Effect, Scientific American, Vol. 214.

[14] Holman, J.P., 1986, Heat Transfer, McGraw Hill, New York.

[15] ISO 230-3, 2001, Machine Tool Test Code – Determination of Thermal Effects, International Organization for Standardization (ISO).

[16] Box, G.E.P., Hunter, W.G., Hunter, J.S., 1978, Statistics for Experimenters, John Wiley & Sons, New York.

[17] AJ Design Pneumatic Mixer Design Calculator, www.ajdesigner.com .